DFT and MP2 Study of the Molecular Structure and Vibrational Spectra of the Anticancer Agent Cyclophosphamide

Hassan M. Badawi and Wolfgang Förner

Department of Chemistry, King Fahd University of Petroleum & Minerals (KFUPM), Dhahran 31261, Saudi Arabia

Reprint requests to W. Förner. Tel.: 966 3 860 3553. Fax: 966 3 860 4277.
E-mail: forner@kfupm.edu.sa

The possible conformations in the most stable structure of cyclophosphamide were investigated at the DFT-B3LYP and MP2/6-311G** levels of calculation. The *axial* structure is calculated to be lower in energy than the *equatorial* form of cyclophosphamide by 5 (MP2) to 6 (DFT) kcal mol^{-1} because of a very weak anomeric effect and weak conjugation. Further it is the same structure as the one found in the X-ray investigations both of the hydrate and of the anhydrous form. The computed DFT vibrational frequencies of the *axial* structure were used to analyze the infrared and Raman spectra using normal-coordinate calculations to provide reliable assignments to the normal modes of the molecule.

Key words: Conformational Structure, Vibrational Spectra, Cyclophosphamide,
N,N-Bis(2-chloroethyl)-1,3,2-oxazaphosphinan-2-amine-2-oxide, Anticancer Agent

Introduction

The conformational stability of vinyl phosphonic dihalides [1] and the acids $F_2PO(OH)$ and $Cl_2PO(OH)$ [2] was investigated as part of a series of phosphorus containing compounds by theoretical DFT-B3LYP and *ab initio* MP2 methods. Vinyl phosphonic difluoride and dichloride were predicted on the DFT-B3LYP/6-311+G** and MP2/6-311+G** levels of theory to exist in *cis* ↔ *gauche* conformational equilibria with the *cis* (phosphonic oxygen eclipses the vinyl group) being the predominant conformer at ambient temperature. The energy difference between the two conformers was calculated to be 1.5 kcal mol^{-1}, with the *cis-gauche* rotational barrier being about 3 kcal mol^{-1} in both molecules [1].

The $F_2PO(OH)$ acid was calculated to exist in a structure in which hydrogen eclipses the phosphoryl PO bond, while the $Cl_2PO(OH)$ acid exists in a structure with an O–P–O–H torsional angle of about 14 and 30° at the DFT-B3LYP and MP2 levels, respectively. The P–O rotational barrier in the two acids was calculated to be about 2 – 3 kcal mol^{-1}, that is significantly lower as compared to the corresponding C–O barrier in carboxylic acids. This low barrier was attributed to the weak covalent character of the P–O bond in the phosphorus containing molecules [2].

As a continuation of studies of structural properties of important organo-phosphorus compounds, the conformational stability of the anticancer agent [3 – 5] cyclophosphamide {*N,N*-bis(2-chloroethyl)-1,3,2-oxaza-phosphinan-2-amine-2-oxide} was studied in the present work. The crystal structure of cyclophosphamide monohydrate has been investigated previously and its molecules were reported to be held together in three dimensions by one N–H···O and two O–H···O hydrogen bonds [6]. Cyclophosphamide is a drug known under various trade names such as Endoxan, Cytoxan, Neosar, Procytox, Revimmune, or Cytophosphane [7]. It is a mustard alkylating agent [8] and used in the treatment of various cancers and autoimmune disorders. It is used against lymphomas, brain cancers, leukemia [9] and solid tumors [10] or also against systemic lupus erythematosis with lupus nephritis [11]. Further it is used to treat severe rheumatoid arthritis [12], Wegener's granulomatosis (under the trade name Cytoxan) [13], and multiple sclerosis (under the trade name Revimmune) [14].

It was concluded that low-dose cyclophosphamide is a candidate for combination therapies, *e. g.* in immunotherapy, with tyrosine kinase inhibitors, and in antiangiogenesis [15]. Actually, cyclophosphamide is not the active substance itself, but is converted in the liver to active metabolites [16].

The energies of possible structures of the molecule were optimized at the DFT-B3LYP and MP2 levels of theory using the extended 6-311G** basis set. Vibrational frequencies of the molecule were also calculated at the DFT-B3LYP level, and vibrational assignments were made on the basis of combined computed (using our PED – Potential Energy Distribution – program) and experimental data.

Computational Details

The program GAUSSIAN 03 [17] running on a 128 node High Performance e-1350 IBM Cluster was used to carry out the calculations. The structure of cyclophosphamide in its *axial* form (Fig. 1) was optimized by minimizing the energy with respect to all the geometrical parameters. The calculated structural parameters of the molecule are listed in Table 1, the energies are given in Table 2. The optimized structural parameters were used to calculate the vibrational wavenumbers of cyclophosphamide in its *axial* structure. A reliable assignment of the fundamentals was proposed on the basis of the combined theoretical [17, 18] and experimental spectra retrieved from the link in ref. [19]. Mainly normal-mode calculations (using our PED – Potential Energy Distribution –
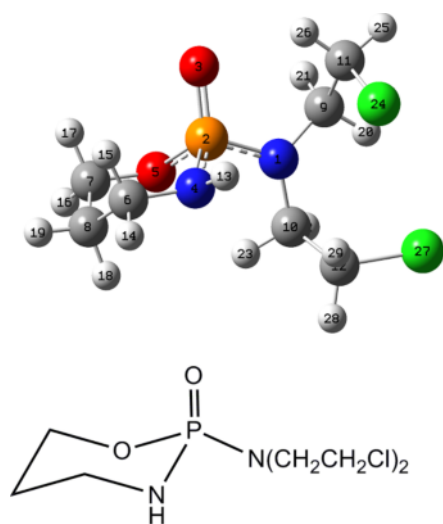
program) were used for this purpose, while the GAUSSVIEW program [18] was used just to give some guidelines. In Table S1 the internal coordinates are shown and in Table S2 the symmetry coordinates used in the normal-mode PED calculations with our program [20]. Note, that the set of internal coordinates is overcomplete in order to facilitate the

Fig. 1. Atom numbering of the *axial* structure of cyclophosphamide and a sketch of the molecular formula.

Table 1. X-Ray (from the monohydrate [6] and the anhydrous form [21]) and calculated structural parameters of the non-hydrogen atoms of the *axial* conformer of cyclophosphamide.

Parameter	B3LYP	MP2	X-Ray diffraction	
			monohydrate	anhydrous
Bond lengths (Å)				
N_1–C_9	1.467	1.461	1.462(6)	1.463(2)
N_1–C_{10}	1.470	1.463	1.463(6)	1.463(2)
P_2–N_1	1.666	1.656	1.630(4)	1.641(2)
P_2–O_3	1.483	1.481	1.470(4)	1.4753(14)
P_2–N_4	1.691	1.684	1.625(5)	1.633(2)
P_2–O_5	1.624	1.622	1.582(4)	1.5881(13)
O_5–C_7	1.448	1.442	1.460(7)	1.462(2)
C_6–N_4	1.483	1.479	1.472(7)	1.478(2)
C_6–C_8	1.529	1.525	1.494(8)	1.514(3)
C_7–C_8	1.524	1.521	1.493(8)	1.518(3)
C_9–C_{11}	1.526	1.526	1.505(7)	1.526(3)
C_{10}–C_{12}	1.528	1.524	1.507(7)	1.514(3)
C_{11}–Cl_{24}	1.819	1.819	1.784(6)	1.789(2)
C_{12}–Cl_{27}	1.819	1.784	1.794(6)	1.791(2)
Bond angles (deg)				
N_1–P_2–N_4	105.4	103.7	106.8(2)	105.84(8)
P_2–N_4–C_6	118.2	116.4	121.9(3)	119.98(13)
P_2–O_5–C_7	118.8	116.3	118.6(2)	117.45(11)
P_2–N_1–C_9	121.6	120.7	121.1(2)	120.41(13)
P_2–N_1–C_{10}	119.5	118.8	121.9(2)	120.04(13)
O_3–P_2–N_1	112.3	112.9	110.0(1)	110.86(8)
O_3–P_2–O_5	115.8	115.4	114.1(1)	112.29(8)
N_4–P_2–N_1	105.4	103.7	106.8(2)	105.84(8)
O_5–P_2–N_1	103.7	104.0	102.4(1)	105.48(8)
O_5–P_2–N_4	100.0	99.9	104.7(1)	101.85(8)
N_1–C_9–C_{11}	110.8	109.9	110.7(3)	112.6(2)
N_1–C_{10}–C_{12}	111.7	111.7	110.8(3)	114.9(2)
N_4–C_6–C_8	110.5	109.8	110.7(3)	109.8(2)
O_5–C_7–C_8	110.2	109.8	110.3(4)	110.11(15)
C_6–C_8–C_7	111.5	110.9	111.3(4)	111.1(2)
C_9–N_1–C_{10}	117.6	116.7	116.8(3)	118.1(2)
Cl_{24}–C_{11}–C_9	110.5	109.9	109.5(3)	108.33(4)
Cl_{27}–C_{12}–C_{10}	110.4	109.9	108.7(3)	111.26(15)
Torsional angles (deg)[a]				
O_3–P_2–N_1–C_{10}	−11.4	−19.9	−1.92	−9.3(2)
P_2–N_1–C_9–C_{11}	−101.4	−106.9	−35.50	−101.8(2)
N_1–C_9–C_{11}–Cl_{24}	182.6	182.2	183.15	179.29(13)
P_2–N_1–C_{10}–C_{12}	−82.5	−76.3	−88.20	−116.1(2)
N_1–C_{10}–C_{12}–Cl_{27}	186.8	185.3	172.60	58.1(2)

[a] A torsional angle A–B–C–D is defined as the angle (the one less or equal than 180°) between the projections of the A–B and C–D bonds on the plane perpendicular to the B–C bond. It is positive when the A to D direction is clockwise.

Structure[a]	B3LYP			MP2		
	(ϕ_1, ϕ_2)	E	ΔE	(ϕ_1, ϕ_2)	E	ΔE
Axial	(79, −77)	−1797.772839	0.000	(79, −77)	−1794.577873	0.000
Equatorial	(−155, 159)	−1797.762706	6.359	(−160, 164)	−1794.570412	4.682

Table 2. Calculated total energies E (hartree) and relative energies ΔE (kcal mol^{-1}) of cyclophosphamide at the DFT-B3LP/6-311G** and MP2/6-311G** levels of theory.

[a] ϕ_1 and ϕ_2 are the torsional angles C_6–N_4–P_2–O_3 and C_7–O_5–P_2–O_3, respectively.

set up of symmetry coordinates. Our program detects and removes redundant internal coordinates automatically [20]. The data of the vibrational assignments are listed in Table 3, while in Table S3 calculated and observed intensity data are listed which were used as a rough guideline in the assignment. Note, that tables incorporated in the Supplementary information, which is available online only, are given a number and the prefix S. The calculated intensity data can only be a guideline, because according to our experience they do not agree too well with observed intensities in many cases. Fig. 2 shows the experimental infrared and Raman spectra of cyclophosphamide monohydrate as retrieved from the link given in ref. [19].

Results and Discussion

Structure

The present study provides a thorough comparison between the X-ray structure of the monohydrate [6] and also of the anhydrous material [21] with the corresponding structure obtained at the DFT-B3LYP/6-311G** and MP2/6-311G** levels of computation. The *equatorial* conformer cannot be the ground state (as found in the calculations; see Table 2) because in the *axial* conformer the lone pairs of the oxygen and the nitrogen atoms in the ring can donate electrons into the antibonding orbitals of the phosphoryl PO group thus stabilizing the system in the *axial* conformer. This effect, although weak, which is rather similar to the common anomeric effect, leads to a weakening of the phosphoryl PO bond and thus to lower wavenumbers of its stretching vibration as compared to phosphonic acid derivatives (see discussion of spectra below). The three stabilizing interactions between the lone pair orbitals on nitrogens and oxygen and the phosphoryl PO bond are visualized by dashed lines in the GAUSSVIEW plots of the structure, indicating that three partial double bonds are formed between the phosphorus atom and the oxygen and nitrogen atoms around it.

Note that Hernández-Laguna *et al*. [22] published a thorough study of the phosphoryl PO bond in several compounds using localized orbitals and also Natural
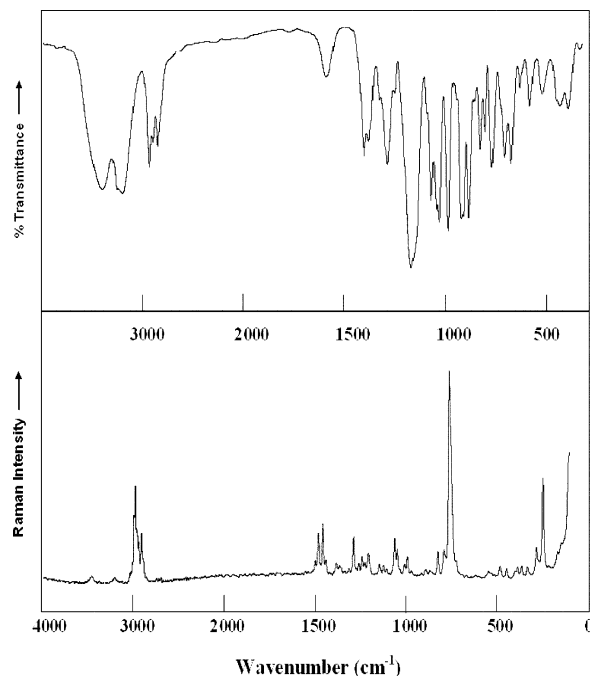

Fig. 2. KBr infrared spectrum (top) and powder Raman spectrum (bottom) of cyclophosphamide monohydrate retrieved from the link given in ref. [19].

Bond Orbitals in which they found that the phosphoryl PO bond is not at all a double bond, but a partially polarized triple bond. Since our calculated properties of the phosphoryl PO bond in cyclophosphamide, such as bond lengths and Mulliken charges, are almost the same as in the systems Hernández-Laguna *et al*. [22] studied, without any doubt also the phosphoryl PO bond in cyclophosphamide, in accordance with previous descriptions, can be taken as a partially polarized strong triple bond [22], leading to rather weak anomeric and conjugation effects. Thus Natural Bond Orbital calculations are not needed to justify these findings. In the *equatorial* form, however, there are only two instead of three of these interactions in the *axial* conformer, because the out-of-ring nitrogen atom is in the wrong geometry. It is interesting to note that the extra-ring nitrogen atom in the *axial* form has a near

planar surrounding (leading to an amide like structure) which is evidence for a weak conjugation with the phosphoryl PO bond.

This conjugation effect leads to the higher stability of the *axial* form, even more than the above discussed anomeric-like effect, while there is nothing like that in the *equatorial* form in which the extra-ring nitrogen atom clearly has a pyramidal surrounding and its lone pair points away from the phosphoryl PO bond. Although these interactions may represent a weak conjugation (also found by Hernández-Laguna *et al.* [22] between a vinyl group and the phosphoryl PO bond), the PO bond has a high ionic character with a Mulliken charge of $+1.26$ on the P and of -0.56 on the O atom, and thus the effects of orbital overlaps will be much weaker than common conjugation effects. A clear indication for the presence of orbital overlaps is the almost planar structure of the PNCC group in the *axial* form, while this group is pyramidal in the *equatorial* form as already mentioned. Further, the out-of-ring PN bond in the *axial* conformer (1.67 Å) is shorter than that in the *equatorial* conformer (1.70 Å). Also the partial charges both on the phosphorus and the extra-ring nitrogen atom in the *equatorial* form indicate reduced conjugation in the higher energy conformer. Sterical hindrance between the chloroethyl groups in the *equatorial* form cannot be ruled out. These effects make the *axial* form by about 6 kcal mol^{-1} (DFT) and by about 5 kcal mol^{-1} (MP2) lower in energy than the *equatorial* one.

The theoretical data in principle represent an isolated molecule that is controlled by intramolecular interactions, while the crystal structure is controlled also by strong intermolecular forces. In the following we want to concentrate on the conformer that is also found in the two X-ray diffraction investigations [6, 21]. The primary objective of the study is to compare the X-ray structure of the solid to the theoretical structure (which best represents an isolated molecule). The comparison shall also be used to determine the limitations of the computed parameters for a description of the molecular structure of the system as found in the solid.

Table 1 indicates that most of the bond lengths calculated with DFT and MP2 are not much different from each other and agree rather well with the experimental ones [6, 21]. Only those for the PO and PN bonds are somewhat smaller in experiment, which might be due to hydrogen bonding interactions in the crystalline hydrate [6] or intermolecular interactions in the anhy-

drous form [21]. The CCl bonds are calculated longer than measured. This is probably due to the lack of diffuse functions in our basis set, but since it seems to concern only CCl bond lengths, this lack of diffuse functions is obviously not very crucial. However, in a highly correlated system like ours the use of a valence triple zeta basis with polarization functions is necessary. The Gaussian basis sets with diffuse functions as implemented in the program are not well balanced and lead to basis set linear dependencies, making calculations with them not very useful (see the comparative calculation published in [23]). There is no well balanced valence triple zeta basis set with polarization and diffuse functions at our hands. However, obviously the lack of diffuse functions influences only CCl bond lengths. Most of the bond angles are again in fair agreement between our calculations and the experimental values. MP2 and DFT values differ generally very little. Rather large differences of about 6 degrees between theory and experiment are found for the P_2–N_4–C_6 and the O_5–P_2–N_4 bond angles. In the former case the DFT value is even better than the MP2 one. The discrepancies are due to interactions between the rather highly charged P, O and N atoms and their environment. Dihedral angles are more different from the experimental values than bond angles. Here one has to take into consideration that the crystalline environment has a larger influence on dihedral angles than on other geometrical parameters.

We tried to find previous theoretical studies of the conformers of cyclophosphamide in several data bases, but with not much success. Two of them dealt explicitly with the preferred conformations of cyclophosphamide and date from 1996 [24] and 1973 [25]. Both were using just semiempirical methods like AM1, PM3 and CNDO, and their results agree with our finding of a chair conformation of the six-membered ring with the phosphoryl PO bond in *axial* position. Another study dealt more with the reactivity of mustard and phosphorus compounds [26], but used also semiempirical methods.

Discussion of vibrational spectra

The vibrational wavenumbers of the *axial* conformation were then calculated at the B3LYP/6-311G** level (Table 3). The molecule has C_1 symmetry and the 81 vibrational modes span the irreducible representation A and should be polarized in the Ra-

Observed[a] Infrared	Raman	Calculated	Obs./Calc.	PED
3426 vs	3435 vvw	3547	0.97	100% NH str (S_{49})
3224 vs	most probably OH stretches in the lattice water molecules			
	3185 vvw	3162	1.01	54% CH$_2$(Cl) asym str iph (S_{12})
				37% CH$_2$(Cl) asym str oph (S_{30})
	2999 sh	3094	0.97	79% CH$_2$(Cl) sym str iph (S_5)
				17% CH$_2$(Cl) sym str oph (S_{23})
	2970 sh	3074	0.97	33% γ-CH$_2$ asym str (S_{43})
				29% γ-CH$_2$ asym str (S_{66})
				16% γ-CH$_2$ sym str (S_{44})
				13% γ-CH$_2$ sym str (S_{67})
2964 s	2963 s	3063	0.97	78% CH$_2$ sym str iph (S_1)
				13% CH$_2$ asym str oph (S_{29})
	2950 s	3054	0.97	76% CH$_2$ sym str oph (S_{19})
				14% CH$_2$ asym str iph (S_{11})
2932 s	2927 sh	3035	0.97	37% γ-CH$_2$ sym str (S_{67})
				35% γ-CH$_2$ sym str (S_{44})
				11% γ-CH$_2$ asym str (S_{66})
2890 m	2896 m	2991	0.97	36% γ-CH$_2$ sym str (S_{67})
				33% γ-CH$_2$ sym str (S_{44})
				15% γ-CH$_2$ asym str (S_{43})
				14% γ-CH$_2$ asym str (S_{66})
1636 m		1525	1.07	95% γ-CH$_2$ def (scissor) (S_{53})
	1490 sh	1492	1.00	49% CH$_2$ def (scissor) oph (S_{20})
				33% CH$_2$(Cl) asym def oph (S_{26})
				11% CH$_2$(Cl) sym def oph (S_{25})
	1472 m	1476	1.00	90% δ-CH$_2$ def (scissor) (S_{57})
1453 s	1448 m	1455	1.00	40% NH bend ipl (S_{81})
				33% γ-CH$_2$ wag (S_{55})
				11% γ-CH$_2$ wag (S_{70})
1431 s	1431 sh	1408	1.02	68% CH$_2$ wag iph (S_3)
1380 sh	1373 vw	1382	1.00	70% CH$_2$ twist oph (S_{31})
1340 s	1340 vvw	1330	1.01	69% CH$_2$ twist iph (S_{13})
				20% CH$_2$(Cl) rock iph (S_{16})
1285 sh		1287	1.00	25% CH$_2$(Cl) sym def iph (S_7)
				25% CH$_2$(Cl) sym def oph (S_{25})
				10% CH$_2$(Cl) asym def iph (S_8)
				10% CH$_2$(Cl) asym def oph (S_{26})
	1278 m	1278	1.00	36% CH$_2$(Cl) rock oph (S_{34})
				17% CH$_2$ rock oph (S_{32})
	1249 vw	1243	1.00	51% γ-CH$_2$ twist (S_{56})
				14% γ-CH$_2$ rock (S_{54})
	1232 w	1234	0.99	45% δ-CH$_2$ twist (S_{73})
1227 vvs	1217 w	1226	1.00	19% CH$_2$(Cl) rock iph (S_{16})
				17% NC$_2$ asym str (S_{38})
				17% P=O str (S_{47})
				11% CH$_2$ rock iph (S_{14})
				10% δ-CH$_2$ twist (S_{73})
1130 s		1143	0.99	45% NC$_2$ asym str (S_{38})
				30% CH$_2$(Cl) asym def iph (S_{15})
				13% CH$_2$ twist iph (S_{13})
1106 sh		1106	1.00	38% CH$_2$(Cl) as def oph (S_{33})
				13% ring str def I (S_{50})
1092 vs		1099	0.99	26% ring str def III (S_{76})
				24% ring str def I (S_{50})
				16% CH$_2$(Cl) as def oph (S_{33})
	1051 m	1050	1.00	49% CH$_2$(Cl) rock oph (S_{24})
				33% CC str iph (S_6)
1047 vs	1036 w	1042	1.00	50% CC str iph (S_6)
				29% CH$_2$(Cl) rock oph (S_{24})
987 s		1032	0.96	37% CH$_2$(Cl) asym def iph (S_{15})
				35% CH$_2$ rock iph (S_{14})
				11% NC$_2$ asym str (S_{38})

Table 3. Observed (infrared and Raman) and calculated (B3LYP/6-311G**) vibrational wavenumbers (cm^{-1}) of *axial* cyclophosphamide together with the PED (Potential Energy Distribution, only values larger 10% are given) for assignment.

Table 3. (continued).

Observed[a]		Calculated	Obs./Calc.	PED
Infrared	Raman			
981 sh	985 vw	997	0.98	37 % NC$_2$ sym str (S$_{41}$)
				19 % CH$_2$(Cl) as def oph (S$_{33}$)
				15 % PN str (S$_{48}$)
				14 % CH$_2$ rock oph (S$_{32}$)
975 sh		971	1.00	22 % ring str def IV (S$_{77}$)
				20 % ring str def V (S$_{78}$)
				11 % γ-CH$_2$ rock (S$_{54}$)
950 s	962 w	961	0.99	26 % ring asym bend def (S$_{62}$)
				17 % ring str def I (S$_{50}$)
				16 % δ-CH$_2$ rock (S$_{58}$)
896 m		911	0.98	61 % γ-CH$_2$ rock (S$_{54}$)
				12 % ring str def V (S$_{78}$)
872 m	870 vvw	863	1.01	60 % ring str def II (S$_{51}$)
				11 % δ-CH$_2$ rock (S$_{58}$)
				11 % ring breathing (S$_{52}$)
838 s		821	1.02	31 % ring str def V (S$_{78}$)
				16 % ring sym puckering (S$_{61}$)
				12 % ring breathing (S$_{52}$)
	813 w	795	1.02	21 % PN str (S$_{48}$)
				17 % NC$_2$ sym str (S$_{41}$)
				12 % ring breathing (S$_{52}$)
777 s	779 w	779	1.00	23 % CH$_2$(Cl) rock iph (S$_{16}$)
				21 % CH$_2$ rock iph (S$_{14}$)
				14 % CH$_2$(Cl) rock oph (S$_{34}$)
				12 % CH$_2$ rock oph (S$_{32}$)
747 s	749 vs	741	1.01	56 % CCl str oph (S$_{22}$)
				18 % CCl bend oph (S$_{28}$)
706 w		734	0.96	39 % CCl str iph (S$_4$)
				24 % ring breathing (S$_{52}$)
658 m		704	0.93[b]	34 % CCl str iph (S$_4$)
				11 % ring breathing (S$_{52}$)
598 m		653	0.92[b]	34 % NH wag (S$_{61}$)
				12 % ring breathing (S$_{52}$)
				11 % ring str def II (S$_{51}$)
518 m		567	0.91[b]	38 % ring as bending def I (S$_{62}$)
				22 % NH wag (S$_{61}$)
				14 % δ-CH$_2$ rock (S$_{58}$)
513 m	520 vvw	525	0.98	20 % CCl str oph (S$_{22}$)
				16 % CCC bend oph (S$_{28}$)
				16 % NC$_2$ rock (S$_{37}$)
				12 % PON def (scissor) (S$_{59}$)
472 vw	470 vw	497	0.96	34 % PON rock (S$_{60}$)
				12 % NC$_2$ scissor (S$_{40}$)
	440 vw	447	0.98	32 % ring as bending def II (S$_{79}$)
				12 % PON wag (S$_{74}$)
	380 vvw	398	0.95	34 % ring as bending def II (S$_{79}$)
				30 % PON wag (S$_{74}$)
	345 vvw	352	0.98	26 % ring sym puckering (S$_{63}$)
				19 % PON twist (S$_{75}$)
	310 vvw	302	1.03	32 % ring asym puckering (S$_{64}$)
				20 % ring sym puckering (S$_{63}$)
	267 wm	241	1.11	27 % PON def (scissor) (S$_{59}$)
				20 % CH$_2$(Cl) rock oph (S$_{27}$)
				15 % CH$_2$(Cl) rock iph (S$_9$)
	231 s	229	1.01	57 % CCC bend iph (S$_{10}$)
				15 % CH$_2$(Cl) rock iph (S$_9$)
	150 sh	155	0.97	55 % ring twisting (S$_{80}$)
				31 % PON twist (S$_{75}$)
	115 sh	105	1.10	47 % C$_2$H$_4$Cl torsion iph (S$_{18}$)
				30 % CH$_2$Cl torsion iph (S$_{17}$)

[a] Abbreviations used: sh, shoulder; v, very; s, strong; m, medium; w, weak; str, stretch; def, deformation; sym, symmetric; asym or as, antisymmetric; iph, in phase combination on both ethylchloride subunits; oph out of phase combination on both ethylchloride subunits; ipl, in plane; opl, out of plane; [b] note that in these cases of low-wavenumber vibrations there are relatively large anharmonicities and here in addition, the movements of large parts of the molecule are influenced by the packing in the solid state.

man spectrum of the liquid. Tentative assignments of the normal modes of the molecule were proposed on the basis of the calculated infrared band intensities, Raman activities, depolarization ratios, and the GAUSSVIEW graphical animations [18] as a guideline, normal-mode calculations and reported experimental spectra of cyclophosphamide monohydrate. Unfortunately we are unable to find in SciFinder and other databases any regular paper reporting the experimental spectra, so that we could only retrieve them from the link to the Japanese National Institute of Advanced Industrial Science and Technology as given in ref. [19], which has no details about sample origin or preparation and about authors. The results are listed in Table 3. The following discussion is focused only on the assignments of the most intense spectral features that characterize cyclophosphamide (Fig. 2). Note that there are always small differences between the GAUSSVIEW animations and a PED result since the latter is based on potential energy while the former shows just the atomic motions in a normal mode.

In general most of the experimental normal modes fit nicely with the calculated ones except for a few of the IR results which were in discrepancy as a result of the hydration in the monohydrate. This is true especially for the very strong OH stretching mode at $3224\,\text{cm}^{-1}$ observed in the infrared spectrum due to the water molecules in the lattice of the hydrate. Another very strong infrared feature is the NH stretching mode at $3426\,\text{cm}^{-1}$ (100% PED). The methylene and ring-CH symmetric stretches are strong features both in the infrared (at $2964\,\text{cm}^{-1}$ with 78% PED from in phase CH_2 stretch and at $2932\,\text{cm}^{-1}$ with 83% PED from several γ-CH_2 stretches) and in the Raman ($2950\,\text{cm}^{-1}$ with 76% PED from out of phase CH_2 stretch) spectra. Also strong bands in the infrared spectrum are the methylene wagging modes at $1453\,\text{cm}^{-1}$ (44% PED from γ-CH_2 wags and 40% PED from NH in plane bend) and $1431\,\text{cm}^{-1}$ (68% CH_2 in phase wags) while methylene twists are strong infrared bands at $1340\,\text{cm}^{-1}$ (69% CH_2 in phase twists) and again at $1130\,\text{cm}^{-1}$ containing 30% in phase methylene deformation coupled with 45% NC_2 antisymmetric stretch, and 13% in phase methylene twist.

The phosphoryl PO stretching mode is a very strong band in the infrared at $1227\,\text{cm}^{-1}$ (17% PO stretch coupled with several other modes) while it shows up roughly 60 wavenumbers higher in vinylphosphonic acid [1, 2], due to the weakening of the phosphoryl PO bond by orbital overlaps as described above and because of the highly mixed character of this normal mode. This large degree of mixing is also indicated by the rather large width of this band (Fig. 2). Two very strong bands in the infrared appear at 1092 and $1047\,\text{cm}^{-1}$, the latter being mainly 50% CC in phase stretch, while the former is highly mixed and contains 16% out of phase methylene (at the chlorine atoms) deformations and 50% of two different ring stretching deformations. Note that the Raman lines in the region between 1490 and $779\,\text{cm}^{-1}$ have intensities just between very weak and medium or are shoulders. Further 37% in phase methylene antisymmetric deformation, 35% in phase rock, and 11% NC_2 symmetric stretch ($987\,\text{cm}^{-1}$) and 25% ring asymmetric bending deformation, 17% ring stretching deformation, and 16% δ-methylene rock ($950\,\text{cm}^{-1}$) correspond to strong infrared bands. A further strong band in the infrared spectrum is at $838\,\text{cm}^{-1}$ and has 31% ring stretching deformation, 16% ring pucker, and 12% ring breathing in it. In this system ring deformations can appear with relatively large intensities in the infrared when they involve the hetero-atoms in the ring, leading to appreciable dipole moment changes. The strong band in the infrared at $777\,\text{cm}^{-1}$ is highly mixed, containing four contributions from different methylene rocks. The very strong Raman line at $749\,\text{cm}^{-1}$ which is also strong in the infrared at $747\,\text{cm}^{-1}$ is mainly due to CCl out of phase stretch (56%) with a very small contribution from out of phase CCl bend (18%). The lower lines are all very weak to medium, besides one (see below).

Due to earlier experience with aromatic rings [27], we expect ring breathing lines with rather low intensities in the Raman spectrum because of the electron-rich ring system containing oxygen, nitrogen and phosphorus. As expected, ring breathing appears highly mixed in three Raman lines, a very weak one at $985\,\text{cm}^{-1}$ with only 12% ring breathing mixed with NC_2 symmetric stretch, PN stretch, and out of phase methylene rock, and at 870 and $813\,\text{cm}^{-1}$ with only 11% and 12% ring breathing, respectively. The lowest wavenumber mode in the spectra, besides two shoulders, is a strong line in the Raman spectrum ($231\,\text{cm}^{-1}$) which is mainly a 57% CCC in phase bend combination in the chloroethyl subunits. The shoulders at 150 and $115\,\text{cm}^{-1}$ are 53% ring twisting and 47% in phase chloroethyl torsion, respectively.

Conclusion

In conclusion, the *axial* structure of cyclophosphamide was found at the DFT-B3LYP and MP2 levels of theory to be more stable than its *equatorial* form. The results were compared to the X-ray structure data of the hydrate [6] and of the anhydrous form [21] and found to be in reasonable agreement. Reliable vibrational assignments of the normal modes of cyclophosphamide in its *axial* structure are provided on the basis of combined theoretical DFT and experimental infrared and Raman data. The calculated wavenumbers were found to fit reasonably well the observed ones. No evidence was found for the presence of the high-energy *equatorial* form in the spectra of the molecule, which is not surprising because the calculated low-energy *axial* conformer is solely found in the X-ray structure analyses [6, 21].

Supporting information

Internal coordinates, the symmetry coordinates used in the normal-mode calculations, and calculated and observed intensity data used in the vibrational assignment are given in tabular form as Supporting Information available online (DOI: 10.5560/ZNB.2012-0069).

Acknowledgement

[1] H. M. Badawi, W. Förner, *J. Mol. Struct. (Theochem)* **2001**, *538*, 73 – 89.

[2] H. M. Badawi, *Can. J. Anal. Sc. Spectrosc.* **2006**, *51*, 215 – 224.

[3] C. S. Tam, J. F. Seymour, *Leuk. Lymphoma* **2011**, *52*, 729 – 731.

[4] N. Singh, M. Nigam, V. Ranjan, D. Zaidi, V. K. Garg, S. Sharma, R. Chaturvedi, R. Shankar, S. Kumar, R. Sharma, K. Mitra, A. K. Balapure, S. K. Rath, *Cancer Sci.* **2011**, *102*, 1059 – 1067.

[5] J. Gerecitano, C. Portlock, P. Hamlin, C. H. Moskowitz, A. Noy, D. Straus, P. Schulman, O. Dumitrescu, D. Sarasohn, J. Pappanicholaou, A. Iasonos, Z. G. Zhang, Q. X. Mo, E. Hornlli, C. N. Rojas, A. D. Zelenetz, O. A. O'Connor, *Clin. Cancer Res.* **2011**, *17*, 2493 – 2501.

[6] S. Garcia-Blanco, A. Perales, *Acta Crystallogr.* **1972**, *B28*, 2647 – 2652.

[7] The listed brand names can be found among others in the *National Cancer Dictionary* under „cyclophosphamide": http://www.cancer.gov/drugdictionary?CdrID=39748 (accessed: 01.10.2012).

[8] C. H. Takimoto, E. Calvo in *Cancer Management: A Multidisciplinary Approach*, 11th ed., (Eds.: R. Pazdur, L. D. Wagman, K. A. Camphausen, W. J. Hoskins), CMP Media, London **2008**.

[9] T. D. Shanfelt, T. Lin, S. M. Geyer, *Cancer* **2007**, *109*, 2291 – 2298.

[10] S. D. Young, M. Whissell, J. C. Noble, *Clin. Cancer Res.* **2006**, *12*, 3092 – 3098.

[11] A. D. Steinberg, H. B. Kaltreider, P. J. Staples, *Ann. Intern. Med.* **1971**, *75*, 165 – 171.

[12] A. S. Townes, J. M. Sowa, L. E. Shulman, *Arthritis Rheum.* **1976**, *19*, 563 – 573.

[13] S. N. Novack, C. M. Pearson, *New Eng. J. Med.* **1971**, *284*, 938 – 942.

[14] N. Makhani, M. P. Gorman, H. M. Branson, *Neurology* **2009**, *72*, 2076 – 2082.

[15] T. Nelius, T. Klatte, *Med. Oncology* **2009**, *27*, 363 – 367.

[16] J. L. Cohen, J. Y. Jao, *J. Pharmacol. Exp. Ther.* **1970**, *174*, 206 – 210.

[17] M. J. Frisch, G. W. Trucks, H. B. Schlegel, G. E. Scuseria, M. A. Robb, J. R. Cheeseman, J. A. Montgomery, Jr., T. Vreven, K. N. Kudin, J. C. Burant, J. M. Millam, S. S. Iyengar, J. Tomasi, V. Barone, B. Mennucci, M. Cossi, G. Scalmani, N. Rega, G. A. Petersson, H. Nakatsuji, M. Hada, M. Ehara, K. Toyota, R. Fukuda, J. Hasegawa, M. Ishida, T. Nakajima, Y. Honda, O. Kitao, H. Nakai, M. Klene, X. Li, J. E. Knox, H. P. Hratchian, J. B. Cross, V. Bakken, C. Adamo, J. Jaramillo, R. Gomperts, R. E. Stratmann, O. Yazyev, A. J. Austin, R. Cammi, C. Pomelli, J. W. Ochterski, P. Y. Ayala, K. Morokuma, G. A. Voth, P. Salvador, J. J. Dannenberg, V. G. Zakrzewski, S. Dapprich, A. D. Daniels, M. C. Strain, O. Farkas, D. K. Malick, A. D. Rabuck, K. Raghavachari, J. B. Foresman, J. V. Ortiz, Q. Cui, A. G. Baboul, S. Clifford, J. Cioslowski, B. B. Stefanov, G. Liu, A. Liashenko, P. Piskorz, I. Komaromi, R. L. Martin, D. J. Fox, T. Keith, M. A. Al-Laham, C. Y. Peng, A. Nanayakkara, M. Challacombe, P. M. W. Gill, B. Johnson, W. Chen, M. W. Wong, C. Gonzalez, J. A. Pople, GAUSSIAN 03 (revision E.01), Gaussian, Inc., Wallingford CT (USA) **2004**.

[18] R. Dennington II, T. Keith, J. Millam, K. Eppinnett, W. L. Hovell, R. Gilliland, GAUSSVIEW (version 3.0), Semichem, Inc., Shawnee Mission KS (USA) **2003**.

[19] Experimental spectra retrieved from the link to SDBSWeb (March 1, 2012): http://www.riodb01.ibase.aist.go.jp/riodb/sdbs/ (National Institute of Advanced Industrial Science and Technology, **2011**) no. 15262.

[20] W. Förner, *Int. J. Quantum Chem.* **2004**, *99*, 533 – 555, and refs. cited therein.

[21] P. G. Jones, H. Thönnessen, A. Fischer, I. Neda, R. Schmutzler, J. Engel, B. Kutscher, U. Niemeyer, *Acta Crystallogr.* **1996**, *C52*, 2359 – 2363.

[22] A. Hernández-Laguna, C. I. Sainz-Díaz, Y. G. Smeyers, J. L. G. de Paz, E. Gálvez-Ruano, *J. Phys. Chem.* **1994**, *98*, 1109 – 1116, and refs. cited therein.

[23] B. Galabov, J. P. Kenney, H. F. Schaefer III, J. R. Durig, *J. Phys. Chem.* **2002**, *106a*, 3625.

[24] B. J. Denny, C. H. Schwalbe, *Pharmaceutical Sciences* **1996**, *2*, 29 – 32.

[25] H. Cable, A. Rauch, L. Pedersen, *J. Pharm. Pharmacol.* **1973**, *25*, 509 – 510.

[26] W. Ulmer, *Z. Naturforsch.* **1979**, *34c*, 658 – 669.

[27] H. M. Badawi, W. Förner, A. A. Al-Saadi, *J. Mol. Struct.* **2004**, *938*, 41 – 47.